JVI Journals.ASM.org

Influenza Viruses with Rearranged Genomes as Live-Attenuated Vaccines

Lindomar Pena, Troy Sutton, Ashok Chockalingam, Sachin Kumar, Matthew Angel, Hongxia Shao, Hongjun Chen, Weizhong Li, Daniel R. Perez

Department of Veterinary Medicine, University of Maryland, College Park, and Virginia—Maryland Regional College of Veterinary Medicine, College Park, Maryland, USA

H5N1 and H9N2 avian influenza virus subtypes top the World Health Organization's list for the greatest pandemic potential. Inactivated H5N1 vaccines induce limited immune responses and, in the case of live-attenuated influenza virus vaccines (LAIV), there are safety concerns regarding the possibility of reassortment between the H5 gene segment and circulating influenza viruses. In order to overcome these drawbacks, we rearranged the genome of an avian H9N2 influenza virus and expressed the entire H5 hemagglutinin open reading frame (ORF) from the segment 8 viral RNA. These vectors had reduced polymerase activities as well as viral replication *in vitro* and excellent safety profiles *in vivo*. Immunization with the dual H9-H5 influenza virus resulted in protection against lethal H5N1 challenge in mice and ferrets, and also against a potentially pandemic H9 virus. Our studies demonstrate that rearranging the influenza virus genome has great potential for the development of improved vaccines against influenza virus as well as other pathogens.

The use of viral vectors for the delivery of traceable reporter genes and bioactive molecules has broad applications in the fields of gene therapy and infectious diseases. A number of live recombinant virus vector vaccines have been licensed for veterinary use, and many are in clinical development for humans (1). These vaccines combine positive features of DNA and live-attenuated vaccines. Viral vectors deliver the nucleic acid-encoding antigens into target host cells, with the added advantage of inducing more robust immune responses elicited by limited replication of the viral entity (1). Since the development of reverse genetic methods for segmented negative-sense RNA viruses, influenza A viruses (IAVs) have also been considered potential vaccine vectors (2).

IAVs are single-stranded segmented RNA viruses of negative polarity that belong to the family *Orthomyxoviridae*. In IAVs, 8 RNA segments encode 10 to 12 viral proteins, including two surface glycoproteins, hemagglutinin (HA), and neuraminidase (NA), which are the major targets for neutralizing antibody responses. The engineering of IAVs as vaccine vectors could offer several advantages: (i) IAVs induce strong immune responses systemically and at the mucosal surfaces (3), (ii) influenza virus replication does not have a DNA phase, eliminating safety concerns regarding integration of viral DNA into the host genome, (iii) IAVs have 16 HA and 9 NA subtypes that are antigenically distinct and which undergo constant antigenic drift, making boost vaccinations feasible (4), and (iv) IAVs are well characterized, with attenuated strains already used as vaccines for humans and livestock (5). Unfortunately, most IAV vectors developed to date contain a combination of abortive replication and/or are either unstable or tolerate only short gene inserts (6).

The avian H9N2s and the highly pathogenic avian influenza virus (HPAIV) H5N1 pose a pandemic threat. The development of effective vaccines against these subtypes is an essential component of WHO's global strategy for pandemic preparedness (7). Inactivated vaccines, particularly in the context of HPAIV H5N1, are poorly immunogenic and often require the addition of an adjuvant and boosting to induce protective responses. LAIV vaccines provide broad cross-protective responses and do not require the use of adjuvants (8, 9). However, LAIVs that employ an H5 HA surface gene segment carry the potential for reassortment with seasonal and/or other circulating influenza viruses (10, 11).

In this study, we rearranged the IAV genome and generated influenza virus vectors that stably expressed foreign genes. We successfully recovered avian H9N2 IAV expressing enhanced green fluorescent protein (eGFP), secreted *Gaussia* luciferase (GLuc), and the entire HA open reading frame (ORF) from a prototypic HPAIV H5N1 (A/VietNam/1203/04 [H5N1]) with a deleted polybasic cleavage site. Expression of both HA proteins (H9 and H5) were detected in cells infected with the H9N2 virus expressing the H5 ORF (H9N2-H5). Notably, immunization of mice and ferrets with the H9N2-H5 virus protected against lethal H5N1 challenge. Because the H5 ORF expressed in this construct does not encode a functional genomic RNA, reassortment of the influenza virus H5 HA is very unlikely. Rearranged IAV vectors have great potential for the development of improved vaccines against influenza virus and other pathogenic agents.

MATERIALS AND METHODS

Ethics statement. Vaccination studies were conducted under biosafety level 2 (BSL-2) conditions, whereas challenge with HPAIV H5N1 was performed under animal biosafety level 3 (ABSL-3) conditions approved by the USDA. Animal studies were performed according to protocols approved by the Institutional Animal Care and Use Committee of the University of Maryland. Animal studies adhered strictly to the U.S. Animal Welfare Act (AWA) laws and regulations.

Viruses and cell lines. Human embryonic kidney cells (293-T) were cultured in Opti-MEM I (Gibco, Grand Island, NY) containing 10% fetal bovine serum (FBS) and antibiotics. Madin-Darby canine kidney

Received 12 September 2012 **Accepted** 12 February 2012
Published ahead of print 28 February 2013
Address correspondence to Daniel R. Perez, dperez1@umd.edu.
L.P. and T.S. contributed equally to this article.

doi:10.1128/JVI.02490-12

TABLE 1 Influenza viruses used in this study

Virus	Genome modification	Transgene	Virus subtype	Acronym
A/Guinea fowl/Hong Kong/WF10/99 (H9N2)[a]	None	None	H9N2	wt H9N2
A/VietNam/1203/04 (H5N1)[b]	None	None	H5N1	wt H5N1
Nonrearranged H9N2-ΔNS[c]	NS1 truncation	None	H9N2	ΔH9N2
Rearranged H9N2-ΔNS1-GFP[d]	NS1 truncation and rearrangement	GFP	H9N2	H9N2-GFP
Rearranged H9N2-ΔNS1-GLuc[e]	NS1 truncation and rearrangement	GLuc	H9N2	H9N2-GLuc
Rearranged H9N2-ΔNS1-ΔH5 Orf[f]	NS1 truncation, rearrangement, and modified cleavage site in HA	Modified H5 HA	H9N2-H5	H9N2-H5
Surface genes from ΔH5N1 in nonrearranged H9N2-ΔNS1 backbone[g]	NS1 truncation and modified cleavage site in HA	None	H5N1	ΔH5N1
Rearranged H5N1 wt[h]	Rearrangement	GFP	H5N1	None
H9:pH1N1 reassortant[i]	None	None	H9N1	H9:pH1N1

[a] GenBank accession number 221116.
[b] GenBank accession number 284218.
[c] A/Guinea fowl/Hong Kong/WF10/99 (H9N2) with NS1 truncation at position 99.
[d] A/Guinea fowl/Hong Kong/WF10/99 (H9N2) with NS1 truncation at position 99 with genome rearrangement and expressing GFP.
[e] A/Guinea fowl/Hong Kong/WF10/99 (H9N2) with NS1 truncation at position 99 with genome rearrangement and expressing GLuc.
[f] A/Guinea fowl/Hong Kong/WF10/99 (H9N2) with NS1 truncation at position 99 with genome rearrangement and expressing H5 HA ORF derived from A/VietNam/1203/04 (H5N1) . The polybasic cleavage site present in the H5 HA was modified.
[g] A 2:6 reassortant containing the surface genes of A/Viet Nam/1203/04 (H5N1) and the internal genes A/Guinea fowl/Hong Kong/WF10/99 (H9N2) with NS1 truncation at position 99. The polybasic cleavage site present in the H5 HA was modified.
[h] A 2:6 reassortant containing 6 genes of A/Viet Nam/1203/04 (H5N1) and segments 2 and 8 derived from the rearranged A/Guinea fowl/Hong Kong/WF10/99 (H9N2). Rearranged segment 2 corresponds to PB1-2A-NEP/NS2, and modified segment 8 refers to full-length NS1-2A-GFP.
[i] H9:pH1N1 is a 1:7 reassortant containing a ferret-adapted HA gene originally derived from A/Guinea fowl/Hong Kong/WF10/99 (H9N2) and the remaining 7 genes from A/Netherlands/602/2009 (H1N1) (12).

(MDCK) cells were maintained in modified Eagle's medium (MEM; Sigma-Aldrich, St. Louis, MO) supplemented with 5% FBS (Sigma-Aldrich) and antibiotics.

The H9N2 wild-type (wt) virus and the H9:pH1N1 reassortant have been previously described (12, 13). The HPAIV A/Vietnam/1203/04 (H5N1) (here, H5N1 wt) was a kind gift from Ruben Donis, CDC, Atlanta, GA. Recombinant viruses used in this study were generated from cloned cDNAs and are described below and in Table 1. All the viruses were propagated in 7- to 10-day-old embryonated hen eggs and titrated by using at least one of the following methods: 50% egg infectious dose (EID_{50}), 50% tissue culture infectious dose ($TCID_{50}$), or 50% mouse lethal dose (MLD_{50}).

Generation of recombinant viruses. The eight-plasmid reverse genetic system for H9N2 wt has been previously described, and it is based in the bidirectional plasmid vector pDP2002 (13). The HA and NA genes from the H5N1 wt strain were cloned into the pDP2002 vector. The ΔH5 HA plasmid carries the HA segment from H5N1 wt, which has been further modified by the removal of the encoded polybasic cleavage site. To generate H9N2 wt with deletions in the NS1 gene (ΔH9N2), the NS segment was modified so that it encoded a C-terminal truncated NS1 protein product comprising amino acids 1 to 99 (ΔNS1) and an unmodified NEP/NS2 protein.

Rearrangement of the influenza virus genome was accomplished by expressing the NEP/NS2 protein from a single polypetide downstream of the PB1 gene. Foreign genes of interest were cloned downstream of a full-length or truncated NS1 gene between two AarI cloning sites, so that there was no introduction of exogenous sequences. Three nucleotide mutations were introduced into the full-length NS1 by site-directed mutagenesis to prevent residual splicing and/or NS2 expression. The splicing donor site was modified from G to A at position 56, and a stop codon was inserted early in NS2 and out of frame with NS1 via a C548A mutation (14). As an additional step, the branch point adenosine at position 509 was modified to cytosine. Processing of the PB1-NEP/NS2 and NS1-foreign gene proteins was achieved by the in-frame incorporation of the foot-and-mouth disease virus (FMDV) 2A *cis*-acting hydrolase element (CHYSEL) (15) downstream of PB1 and NS1, respectively. The corresponding packaging signals previously determined for RNA segments 2 and 8 were maintained to achieve efficient viral RNA (vRNA) incorporation into virions (16, 17). All the plasmid constructs and recovered recombinant viruses were fully sequenced to confirm their identities.

Minigenome assay. The minigenome assay was performed as described previously (18). The PB1 attenuated plasmid (PB1 *att*) used here as a control has been previously published and contains the K391E, E581G, and A661T mutations and an HA tag sequence fused in frame with the C terminus of the PB1 protein (13).

Growth kinetics. MDCK cells were seeded in 6-well plates and infected in triplicate at a multiplicity of infection (MOI) of 0.01. Following adsorption for 1 h, the monolayers were washed 3 times with phosphate-buffered saline (PBS), and 2 ml of Opti-MEM containing 1 μg/ml tosyl-sulfonyl phenylalanyl chloromethyl ketone-trypsin (Worthington Biochemical Corp., Lakewood, NJ) was added. Plates were incubated at 37°C, and cell culture supernatants were harvested at 0, 12, 24, 48, 72, and 96 h postinfection (hpi). Viral titers were determined based on the $TCID_{50}$ in MDCK cells.

Immunofluorescence assay. MDCK cells grown in Nunc Lab-Tek II chamber slides (Thermo Fisher Scientific Inc., Waltham, MA) were infected with an MOI of 1 with the viruses indicated below in Fig. 1d. At 12 hpi, cells were fixed with 4% paraformaldehyde solution, washed with PBS, incubated with 0.2% Triton X-100 in PBS, and blocked with 5% bovine serum albumin (BSA). Incubation with the in-house-produced corresponding primary mouse monoclonal antibodies (MAbs; 1:500 dilution in PBS; anti-H5 DPJY01 and anti-H9 3G8, respectively) was followed by incubation with goat anti-mouse–fluorescein isothiocyanate–labeled secondary antibody (Southern Biotech, Birmingham, AL). Cells were visualized using a Zeiss Axiovert 200 M microscope equipped with a Chroma 41001 filter set.

Immunoelectron microscopy. Recombinant viruses were purified by sucrose density gradient centrifugation. Purified viruses were adsorbed to Formvar/silicon monoxide-coated nickel grids (Electron Microscopy Sciences, Hatfield, PA). The grids were blocked in PBS containing 0.2% BSA and incubated with MAbs specific for the H5 or H9 HA (anti-H5 DPJY01 and anti-H9 3G8, respectively). Grids were washed in blocking solution and incubated with goat anti-mouse IgG antiserum conjugated to 6-nm gold beads (Aurion, Costerweg, The Netherlands). The grids were then negatively stained with 2% phosphotungstic acid (PTA) for 3 min, dried, and examined under a transmission electron microscope.

Mouse studies. Five-week-old female BALB/c mice (Charles River Laboratories, Frederick, MD) were anesthetized with isoflurane prior to intranasal inoculation. Mice were vaccinated with 50 μl 10^5 EID_{50} of the recombinant viruses diluted in PBS. A boost immunization was given to half of the animals 2 weeks after the first inoculation. Each experimental group contained 30 animals. Mice were divided into 4 groups as follows: (i) PBS (negative control); (ii) H9N2-GFP (vector control); (iii) H9N2-H5 (test vaccine); (iv) ΔH5N1 (positive control for the H5N1 vaccine). At 2 weeks postvaccination (or 2 weeks postboost for animals immunized twice), each group was divided into 3 subgroups ($n = 10$) and intranasally challenged with either 20, 200, or 2,000 MLD_{50} of the HPAIV H5N1 strain. Mice were bled using the submandibular bleeding method (19) prior to inoculation and at several time points after immunization to evaluate the immunogenicity of the vaccines. At 5 days postchallenge (dpc), 3 mice from each subgroup were euthanized and their lungs were collected to measure levels of challenge virus. Tissue homogenates were prepared in PBS, clarified by centrifugation, and stored at −70°C until use. Clinical signs of disease, body weight, and mortality were monitored daily throughout the experiment to evaluate vaccine safety and efficacy. Mice presenting ≥20% body weight loss were humanely euthanized and counted as having succumbed to the infection.

Alternatively, 5 groups of mice ($n = 8$) consisting of the same treatment groups as above and an additional ΔH9N2 virus control were immunized twice intranasally (2 weeks apart) with 10^5 EID_{50}/mouse. At 2 weeks postboost, animals were challenged with 10^6 $TCID_{50}$/mouse of the H9:pH1N1 reassortant virus (12). Four animals from each group were euthanized at 3 dpc, and the remaining 4 animals were euthanized at 5 dpc for virus titration of the lungs.

Ferret studies. Eighteen female Fitch ferrets, 3 to 6 months old, were purchased from Triple F Farms (Sayre, PA) and divided into 4 groups (i) PBS (negative control) ($n = 3$); (ii) H9N2-GFP (vector control) ($n = 6$); (iii) H9N2-H5 (test vaccine) ($n = 6$); (iv) ΔH5N1(positive control) ($n = 3$). All ferrets were seronegative for IAV. Prior to vaccination, ferrets received a subcutaneous implantable temperature transponder (Bio Medic Data Systems, Seaford, DE) and were monitored for 5 to 7 days to measure body weight and establish baseline body temperatures. Ferrets were intranasally immunized twice, 2 weeks apart, with 1 ml containing 10^6 EID_{50} of the recombinant virus diluted in PBS. At 2 weeks postboost, ferrets were challenged with a lethal dose (10^6 EID_{50}) of the HPAIV H5N1 A/Vietnam/1203/2004 strain. Body weight changes, clinical signs of disease, including fever and mortality, were monitored daily throughout the experiment. Nasal washes were collected for 9 dpc to quantify virus shedding. Blood samples were collected at 0, 14, and 28 days postvaccination (dpv). After challenge, blood was collected from surviving ferrets on days 14 and 21.

Chicken studies. Two-week-old specific-pathogen-free leghorn chickens were inoculated intravenously ($n = 2$) (Table 1) or through a combination of natural routes ($n = 5$/group; intranasal, intraocular, oral, and intratracheal) with 10^7 EID_{50} of the rearranged HPAIV H5N1. Morbidity and mortality were followed for 10 days after inoculation.

Statistical analysis. Statistical analyses were performed using GraphPad Prism software version 5.00 (San Diego, CA). Comparisons between two treatment means were achieved using a two-tailed Student *t* test, whereas multiple comparisons were carried out by analysis of variance (ANOVA) using Tukey's *post hoc* test, unless otherwise specified. The differences were considered statistically significant at a P level of <0.05.

RESULTS

Generation of influenza virus vectors with rearranged genomes expressing reporter genes. The IAV RNA segment 8 codes for two proteins: NS1, a nonstructural protein that inhibits the host's antiviral response, and NEP/NS2, a structural protein involved in viral assembly and gene regulation. NS1 is produced from an unspliced mRNA, whereas NEP/NS2 is expressed from a spliced mRNA (20). Here, we used reverse genetics to rearrange the genome of an avian IAV, A/Guinea Fowl/Hong Kong/WF10/99 (H9N2) (13) (here referred to as wt H9N2). We chose this strain because it grows well in eggs and tissue culture and has been shown to replicate in several animal species, such as mice, chickens, and ferrets, without previous adaptation (13, 21). In addition, we previously showed that LAIVs based on the wt H9N2 background have adequate attenuation and protection efficacy profiles (13, 21, 22).

Rearrangement of the influenza virus genome was accomplished by expressing the NEP/NS2 ORF from a single polypeptide downstream of the PB1 gene. Introducing the FMDV 2A autoproteolytic cleavage site between the PB1 and NEP/NS2 ORFs allowed cotranslational release of the latter from the upstream PB1-2A chimeric protein (Fig. 1a). Removing the NEP/NS2 gene from RNA segment 8 resulted in additional cloning space in this segment. The expression of the transgene of interest was achieved by cloning it downstream of either a full-length or a truncated NS1 gene (NS1-99aa, expressing the first N-terminal 99 amino acids). The FMDV 2A was cloned between NS1 and the transgene to enable discrete expression of the foreign protein. To prevent any residual splicing activity, the donor site and branch point within full-length NS1 were mutated, and a stop codon was inserted early in the residual open reading frame of NS2 (14). The corresponding packaging signals previously determined for RNA segments 2 and 8 were maintained to optimize incorporation of the modified viral ribonucleoprotein particles (vRNPs) into virions (16, 17). As proof of principle for this approach, the GFP and the GLuc transgenes were cloned into this vector, ultimately resulting in virus rescue (Fig. 1; details of the virus constructs are described in Table 1). These recombinant IAVs reached titers on the order of 6 to 7 $\log_{10}$ EID_{50}/ml after amplification in embryonated eggs, and transgene expression was maintained for up to 10 passages (data not shown). Expression of GFP and GLuc reporter genes was readily detected in the cytoplasm and supernatant, respectively, of infected MDCK cells (Fig. 1b and c).

The H5 HA expressed from segment 8 is incorporated into the envelope of the rearranged H9N2 vector. A rearranged IAV vaccine vector was developed in which the HA ORF from H5N1 was cloned downstream of a truncated NS1 gene (NS1-99aa) in the rearranged H9N2 vector (Fig. 1d). A ΔH5 HA was used with a monobasic cleavage site as previously described (23). The recombinant H9N2-H5 virus was successfully recovered and propagated in embryonated eggs. Cells infected with the H9N2-H5 virus expressed high levels of both HA subtypes as determined by immunofluorescence assay (IFA) with HA subtype-specific MAbs (Fig. 1d).

Previous studies demonstrated the surface incorporation of two different HAs (H1 and H3 subtypes) by a recombinant influenza virus containing 9 RNA segments (24). We next sought to determine whether the H5 HA could be incorporated into virions. The H9N2-H5 virus showed typical influenza virus morphology, consisting of pleomorphic particles and roughly spheroidal virions of approximately 100 nm in diameter. Immunogold electron microscopy using anti-H5- and anti-H9-specific MAbs revealed that both HAs were incorporated into the envelope of the H9N2-H5 virus. As expected, H5 and H9 control viruses only reacted with the respective MAb (Fig. 1d). These results indicated that rearranged IAV vectors retained the typical virion morphology and that both HA proteins were incorporated into the eight-segmented H9N2-H5 rearranged vector.

Genome rearrangement leads to impaired polymerase activity and reduced viral growth *in vitro*. To study the effects of

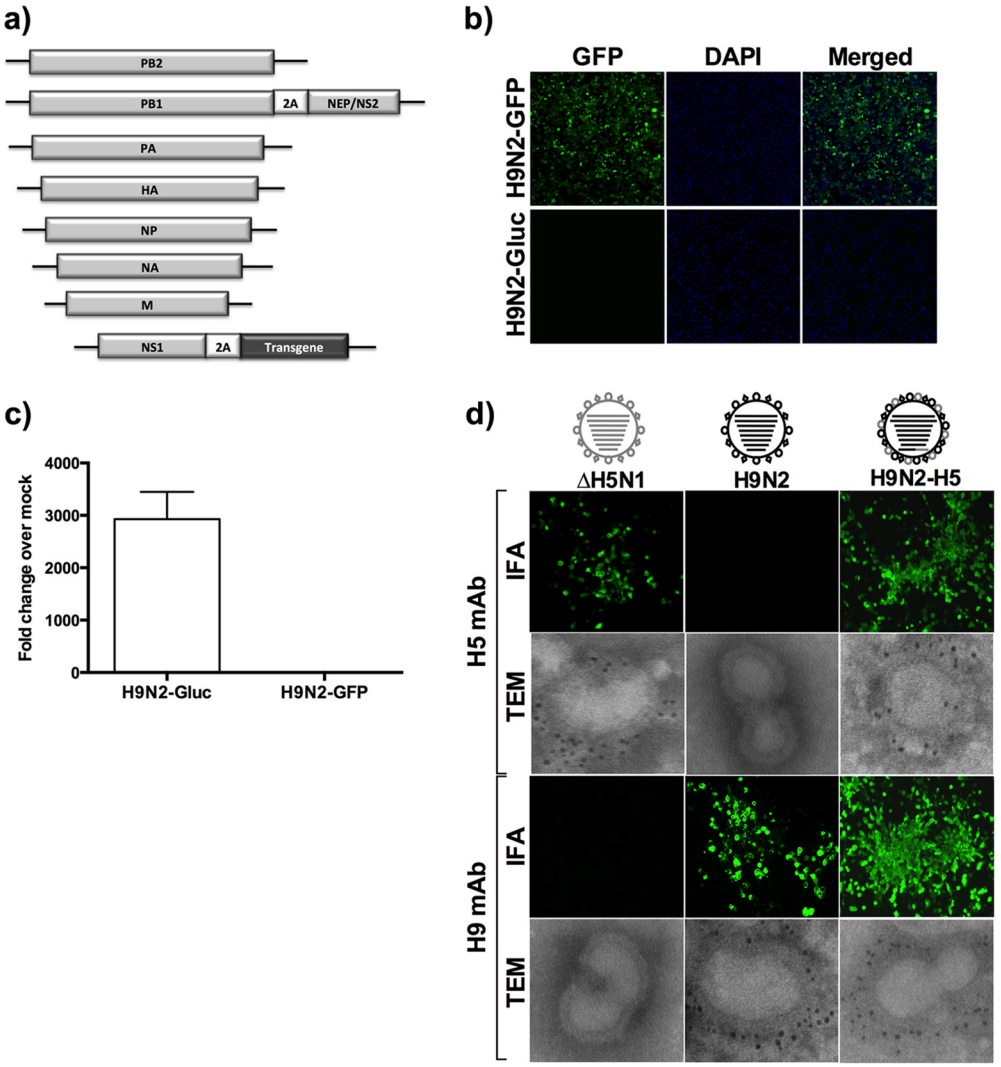

FIG 1 Rearranged H9N2 influenza A viruses expressing foreign genes. (a) Schematic representation of rearranged influenza viruses. NEP/NS2 protein is expressed from a single ORF (solid box) downstream of the PB1 gene, whereas the foreign gene of interest is expressed downstream of a C-terminal truncated NS1 gene (expressing only the first 99 amino acids). The packaging signals span both the untranslated region (solid line) and part of the ORF at both ends of each RNA segment. Recombinant H9N2 viruses were made to express either eGFP (b) or secreted GLuc (c), or the H5 HA ORF (d). The viruses were rescued by reverse genetics and used to infect MDCK cells. At 24 hpi, GFP expression was detected by fluorescence microscopy (b) and GLuc was detected in the tissue culture supernatant in a luficerase assay with the BioLux Gaussia luciferase assay kit (NEB) (c). Expression levels of the H9 and the H5 HA proteins were confirmed by IFA and transmission electron microscopy (TEM) with monoclonal antibodies specific for these antigens and compared to wt H5 and H9N2 viruses, respectively. In the TEM images, black dots correspond to immunogold reactions to either H5 or H9 HA proteins. Note the incorporation of H5 HA into virus particles (d). DAPI, 4′,6-diamidino-2-phenylindole.

genome rearrangement on viral polymerase activity, we performed a minigenome assay as previously described (18). The presence of PB1-2A-NEP/NS2 led to significantly lower polymerase activities than with the wt PB1 gene at different temperatures (Fig. 2a). These results suggest that the strategy used to rearrange the IAV genome decreases viral polymerase activity.

To evaluate whether the reduction in polymerase activity would result in decreased virus replication, the growth properties of the rearranged H9N2-GFP and H9N2-H5 viruses was evaluated in MDCK cells infected at an MOI of 0.01. In agreement with the minigenome assay results, rearranged viruses harboring a truncated NS1 had 10- to 100-fold reductions in virus titers compared to nonrearranged viruses containing the same NS1 deletion. Both wt and rearranged viruses reached maximum viral titers at 24 hpi (Fig. 2b). Together, these results indicate that rearranged viruses can undergo multiple cycles of replication in MDCK cells, although peak titers are at least 10-fold less than with wt isogenic virus.

Genome rearrangement strongly attenuates influenza virus vectors *in vivo*. To evaluate the safety profile of the rearranged IAV vectors, we performed studies in mice, ferrets, and chickens. BALB/c mice were intranasally inoculated with 10^5 EID_{50}/mouse of either H9N2-GFP or H9N2-H5 rearranged vectors. Additional groups included a PBS control, a nonrearranged ΔH5N1 virus (containing the surface genes derived from a low-pathogenicity A/Vietnam/1203/04, with its polybasic cleavage site in HA removed, in the background of the NS1-truncated H9N2 wt virus), a nonrearranged ΔH9N2 virus (NS1-truncated H9N2 wt virus), and the wt H9N2 virus (Table 1).

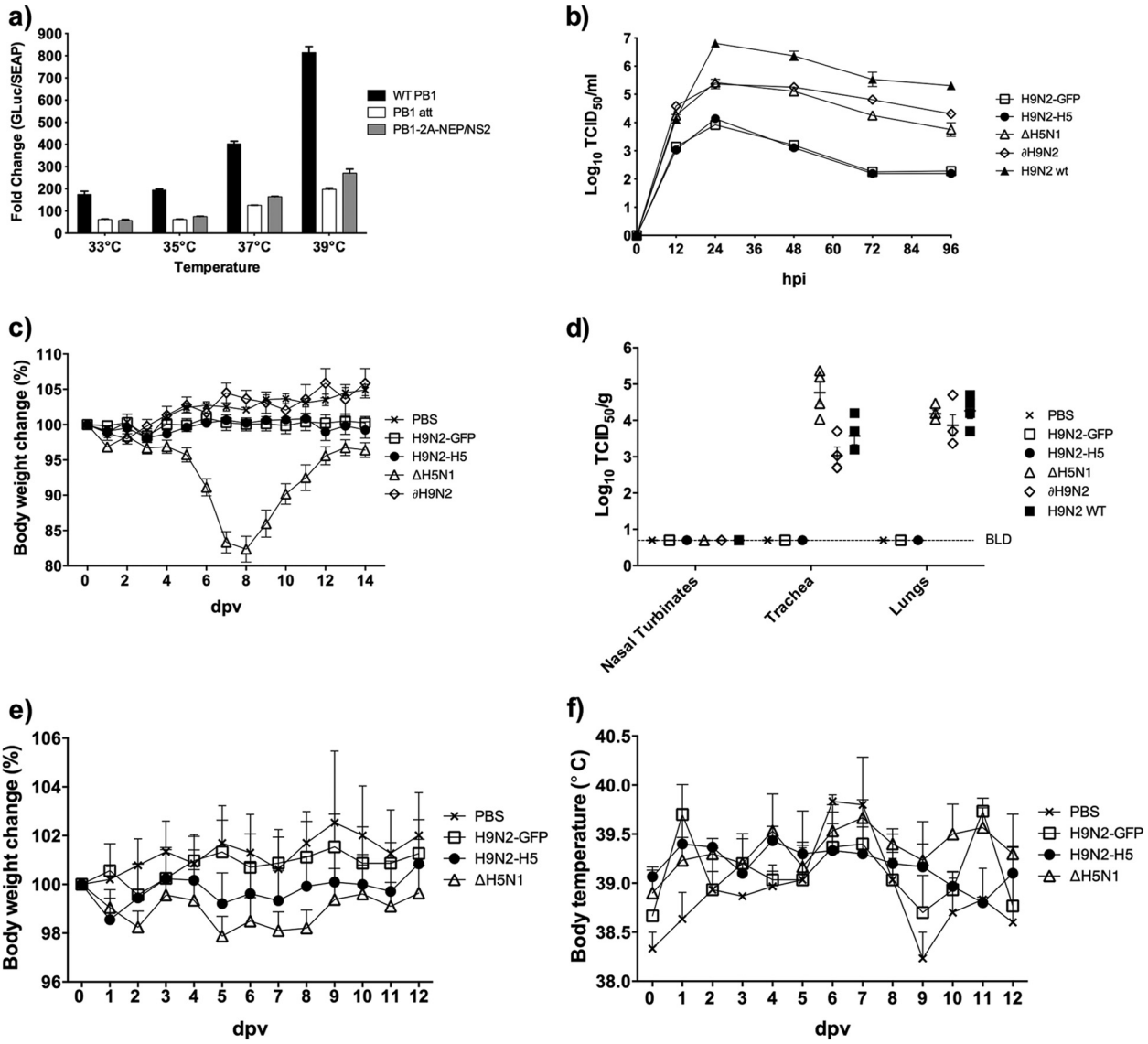

FIG 2 *In vitro* characterization and *in vivo* attenuation of rearranged influenza vectors. (a) Minigenome assay. 293-T cells were grown to 80% confluence in 6-well plates, transfected with 1 μg each of the influenza virus driven-luciferase reporter plasmids (GLuc) and PB2, PB1, PA, and NP plasmids, and incubated at different temperatures, as shown. pCMV/SEAP, which carries the secreted alkaline phosphatase gene was cotransfected into the cells to normalize transfection efficiency. The wt PB1 and an attenuated PB1 gene (PB1 att) were used here as controls. At 24 h posttransfection, the supernatant was harvested and assayed for both luciferase and phosphatase activities. Normalized polymerase activities (means ± standard errors [SE]) were determined from three independent experiments. (b) Multicycle step growth curve. MDCK cells were seeded in 6-well plates and infected in triplicate with each of the viruses described in Table 1 at an MOI of 0.01. Supernatants were harvested at the indicated time points and titrated in MDCK cells based on the $TCID_{50}$. Data are shown as the means ± SE. (c) Safety studies in mice. Body weight changes following intranasal inoculation of BALB/c mice ($n = 10$) with 10^5 EID_{50}/mouse of the recombinant viruses. (d) Viral replication in the respiratory tracts of mice. BALB/c mice ($n = 4$) were inoculated with 10^5 EID_{50}, and viral titers in the indicated organs at 3 dpi were determined based on the $TCID_{50}$. The lower limit of detection (0.6 $TCID_{50}$/ml) of the assay is indicated by the dashed horizontal line. (e and f) Attenuation in ferrets. Ferrets ($n = 3$) were intranasally inoculated with 10^6 EID_{50}/animal with the recombinant viruses, and body temperature (e) and body weight (f) were recorded daily. Data are shown as the mean ± SE.

Vaccination of mice with the rearranged H9N2 vectors produced no clinical disease signs, and there was no change in body weight. Conversely, mice inoculated with the ΔH5N1 virus showed significant body weight loss (≤20%) by 8 dpi, although they eventually recovered (Fig. 2c). In examining tissue tropism and viral replication at 3 dpi, the rearranged H9N2 vectors were not detected in the respiratory tract, whereas ΔH5N1 and ΔH9N2 replicated to high virus titers in the respiratory tracts of mice (Fig. 2d). A similar study conducted in ferrets confirmed the safety features of rearranged viruses as determined by the absence of clinical signs of disease (Fig. 2e and f and data not shown).

Because the H5 HA is expressed from the H9N2-H5 virus as a chimeric HA segment with the packaging signals of the NS gene, the possibility of reassortment of the H5 HA is remote (25). Nevertheless, genetic reassortment could take place if a circulating IAV exchanged both RNA segments 2 and 8 with the rearranged IAV. Therefore, we addressed this question by rescuing an H5N1 virus containing 6 wt RNA segments (1, 3, 4, 5, 6, and 7) from the

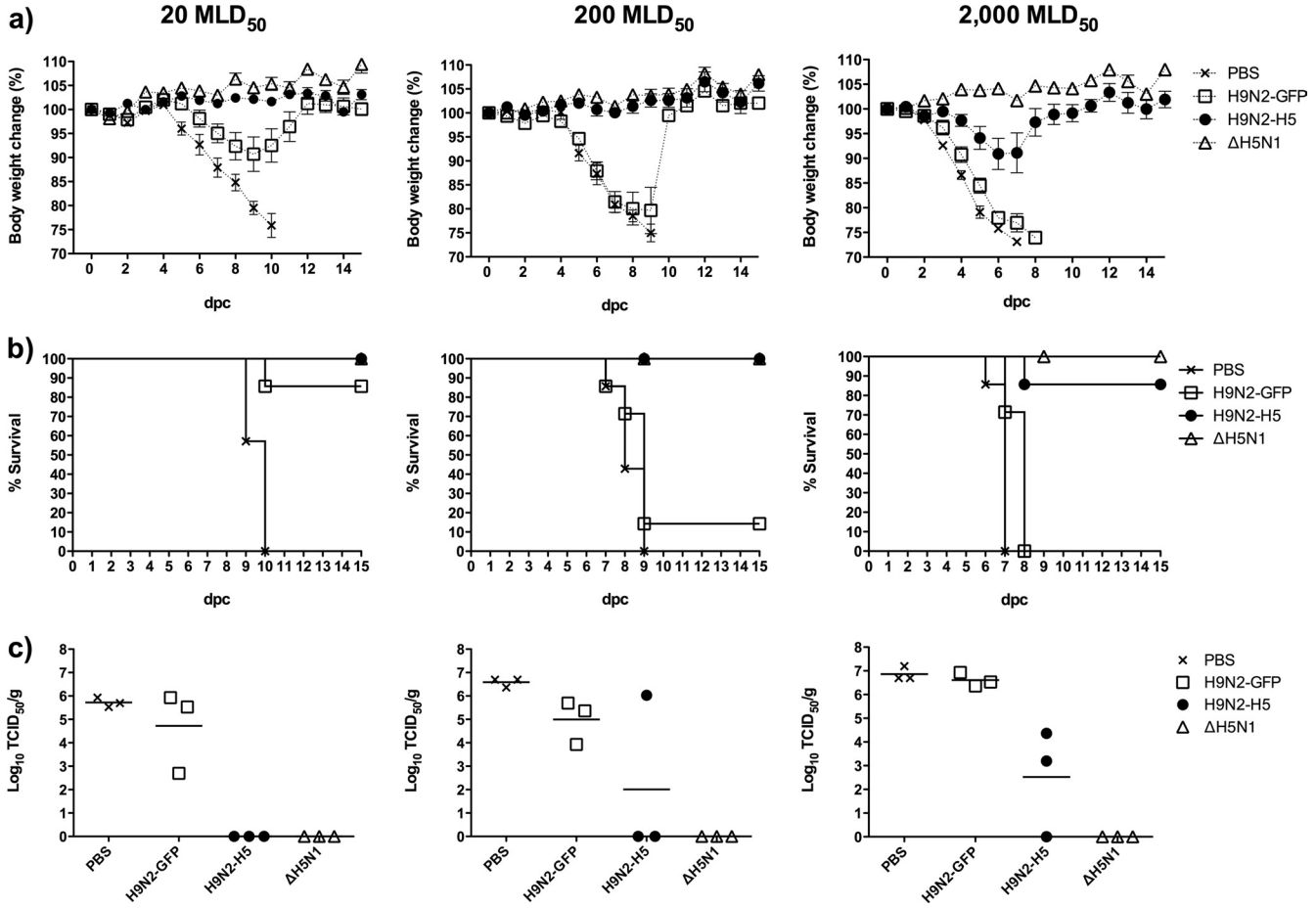

FIG 3 Protective efficacy of the H9N2-H5 rearranged influenza virus vector against HPAIV H5N1 challenge in mice after a single immunization. BALB/c mice ($n = 30$) were intranasally vaccinated with 10^5 EID_{50}/mouse of the recombinant virus. At 2 weeks postvaccination, each treatment group was divided into 3 subgroups ($n = 10$) and challenged with either 20 (left column), 200 (middle column), or 2,000 (right column) MLD_{50} of the virulent H5N1 strain by the intranasal route. The graphs show the percent body weight change ($n = 7$) (a), survival ($n = 7$) (b), and virus titers (mean ± SEM of $\log_{10}$ $TCID_{50}$/gram) in lung homogenates ($n = 3$) (c).

HPAIV H5N1 strain and 2 segments (PB1-2A-NEP/NS2 and NS1-2A-GFP, encoding a full-length NS1) derived from the rearranged H9N2 virus. The pathogenicity of the rearranged HPAIV H5N1 was evaluated in chickens. Leghorn chickens were inoculated intravenously or through natural routes with a total of 10^7 EID_{50} of the rearranged HPAIV H5N1 and followed clinically. None of the chickens died or developed clinical signs of disease upon inoculation (data not shown). In comparison to our previous studies with wt HPAI H5N1, in which 10^6 EID_{50} was highly lethal (13), these findings suggested that even if the rearranged virus reassorted with a HPAIV H5N1, the resulting virus would be completely attenuated. Together, these results indicate that rearranged-based IAV vectors exhibit desirable safety features in three animal species.

Rearranged H9N2-H5 virus provides protection against lethal H5N1 challenge. The ability of the rearranged H9N2-H5 virus to induce protective immune responses was assessed in mice and ferrets. BALB/c mice were intranasally vaccinated once (Fig. 3) or twice (Fig. 4) with 10^5 EID_{50}/animal with one of the following treatments: (i) PBS (negative control); (ii) H9N2-GFP (vector control); (iii) H9N2-H5 (test vaccine); (iv) ΔH5N1 (positive control for the H5N1 vaccine). At 2 weeks postvaccination (or 2 weeks postboost for animals immunized twice), each group ($n = 30$) was divided into 3 subgroups ($n = 10$) and challenged with either 20, 200, or 2,000 MLD_{50} of the H5N1 strain. Three mice from each subgroup were euthanized at 5 dpc to evaluate the levels of challenge virus replication. A single dose of the H9N2-H5 vector provided complete protection from morbidity and mortality following challenges with 20 or 200 MLD_{50} of HPAIV H5N1 (Fig. 3). The subgroup challenged with 2,000 MLD_{50} lost an average of ≤10% of body weight by 7 dpc, but the animals recovered, with the exception of a single mouse that succumbed to infection (Fig. 3a). In contrast, the group singly immunized with the H9N2-GFP vector was not fully protected, since all animals developed clinical disease and lost body weight with any challenge dose. The mortality rate for the H9N2-GFP group was 14%, 86%, and 100% for the 20, 200, and 2,000 MLD_{50} challenge doses, respectively (Fig. 3b). Protection against pulmonary viral replication mirrored the clinical performance of the H9N2-H5 vaccine (Fig. 3c).

Importantly, a second dose or boost with the H9N2-H5 vaccine resulted in complete clinical protection and sterilizing immunity in all individuals, regardless of the challenge dose used (Fig. 4). In the H9N2-GFP group, boost vaccination elicited protection from morbidity against 20 MLD_{50} challenge. However, these animals had approximately 10^3 $TCID_{50}$ of virus/g of lung

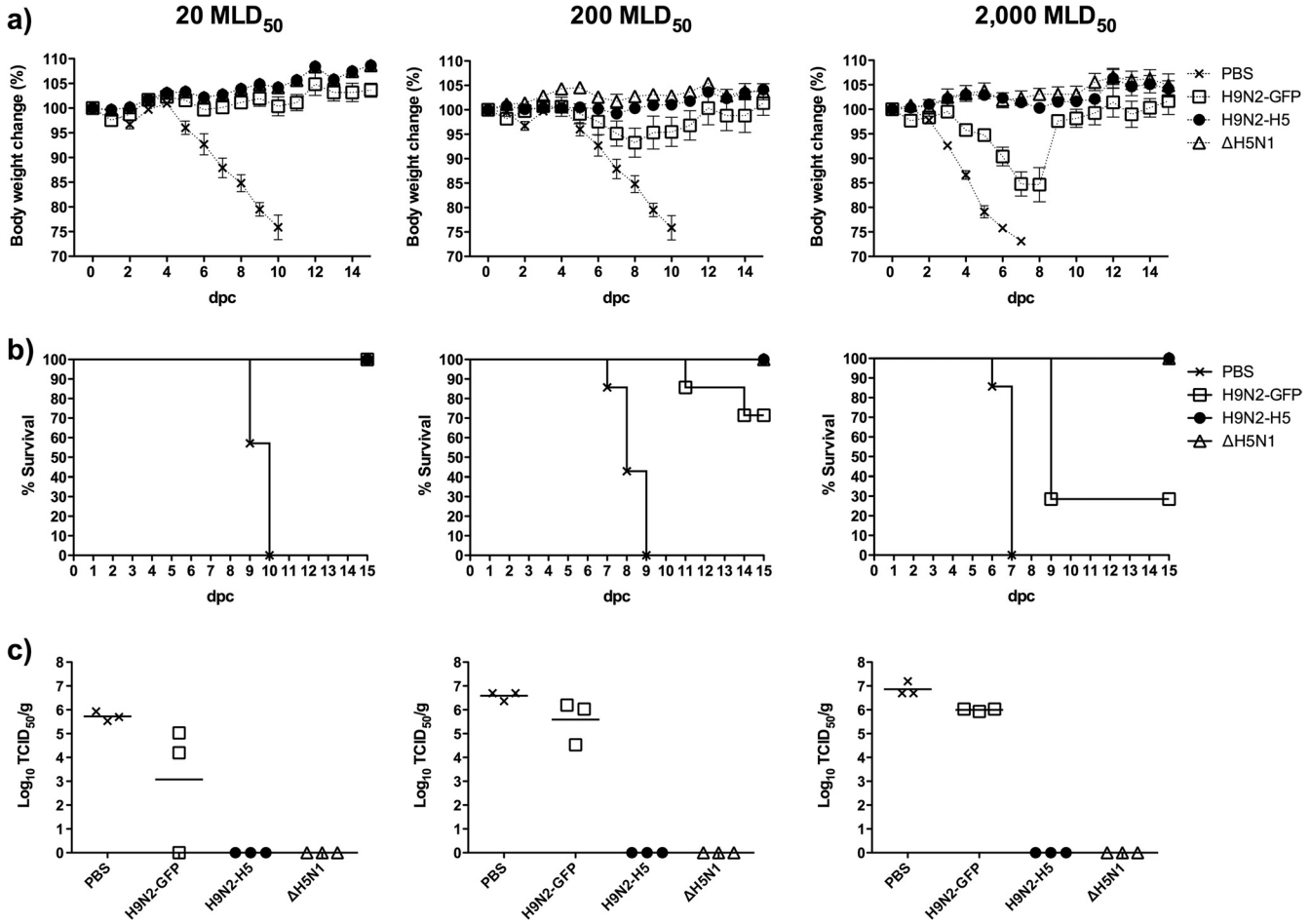

FIG 4 Protective efficacy of the H9N2-H5 rearranged influenza virus vector in mice against HPAIV H5N1 challenges after boost immunization. BALB/c mice ($n = 30$) were intranasally inoculated with 10^5 EID_{50}/mouse of the recombinant viruses and similarly at 2 weeks postvaccination. At 2 weeks postboost, each treatment group was divided into 3 subgroups ($n = 10$) and challenged with either 20 (left column), 200 (middle column), or 2,000 (right column) MLD_{50} of the virulent H5N1 strain by the intranasal route. The graphs show the percent body weight change ($n = 7$) (a), survival ($n = 7$) (b), and virus titers (means ± SEM of $\log_{10}$ $TCID_{50}$/gram) in lung homogenates ($n = 3$) (c). The PBS control group in panel c is the same group for which results are shown in Fig. 3c. This group is included here, as a PBS boost was not expected to result in increased protection.

tissue. Challenge with 200 and 2,000 MLD_{50} overcame the cross-protective immunity induced by the H9N2-GFP vector, as indicated by 29% and 72% mortality rates, respectively, and high levels of replicating challenge virus in the lungs (10^5 to 10^6 $TCID_{50}$ of virus/g of lung) (Fig. 4c). Importantly, the H9N2-H5 vaccine also provided sterilizing immunity in mice challenged with an avian H9-pandemic H1N1 reassortant virus consisting of a ferret-adapted H9N2 HA and the remaining 7 genes from pH1N1 (12) (data not shown). Collectively, these results demonstrate that the rearranged H9N2-H5 vector is suitable for prime/boost vaccination protocols and protects against H5 and H9 challenges.

To gain more insight into the efficacy of the H9N2-H5 vector, we conducted a vaccine-challenge study in ferrets, an established model of IAV (26) (Fig. 5). Ferrets were vaccinated intranasally twice on days 0 and 14 with 10^6 EID_{50} of virus/animal and challenged at 2 weeks postboost with 10^6 EID_{50} of H5N1. This challenge was extremely severe (equivalent to 10,000 times the 50% ferret lethal dose [27]) and was chosen with the objective to discriminate the protective responses induced by the H9N2-H5 vector from the cross-protection induced by the H9N2-GFP vector control. Following challenge, PBS-vaccinated animals had high levels of viral replication (Fig. 5), and all control animals succumbed to infection or were euthanized by day 7 postchallenge. These animals developed severe clinical disease, which was characterized by fever, lethargy, anorexia, severe body weight loss, and diarrhea. The ΔH5N1-vaccinated ferrets did not show clinical signs of disease after challenge, although a low level of virus shedding was detected in the nasal wash from one ferret on day 3 (Fig. 5). All ferrets vaccinated with the H9N2-H5 virus were completely protected against death and disease. In contrast, all of the ferrets in the H9N2-GFP group developed severe clinical infection, showing weight loss and viral shedding. Furthermore, 5 of 6 ferrets in the H9N2-GFP group succumbed to the infection. In the H9N2-GFP group, the single ferret that survived challenge shed large amounts of virus and had a maximal body weight loss of 18%. On day 3 postchallenge, the protected H9N2-H5 ferrets had a 100-fold reduction in viral shedding compared to the ferrets in the H9N2-GFP group, and by day 5 none of the H9N2-H5 ferrets was shedding virus. Interestingly, although each ferret vaccinated with either the H9N2-H5, H9N2-GFP, or ΔH5N1 viruses showed

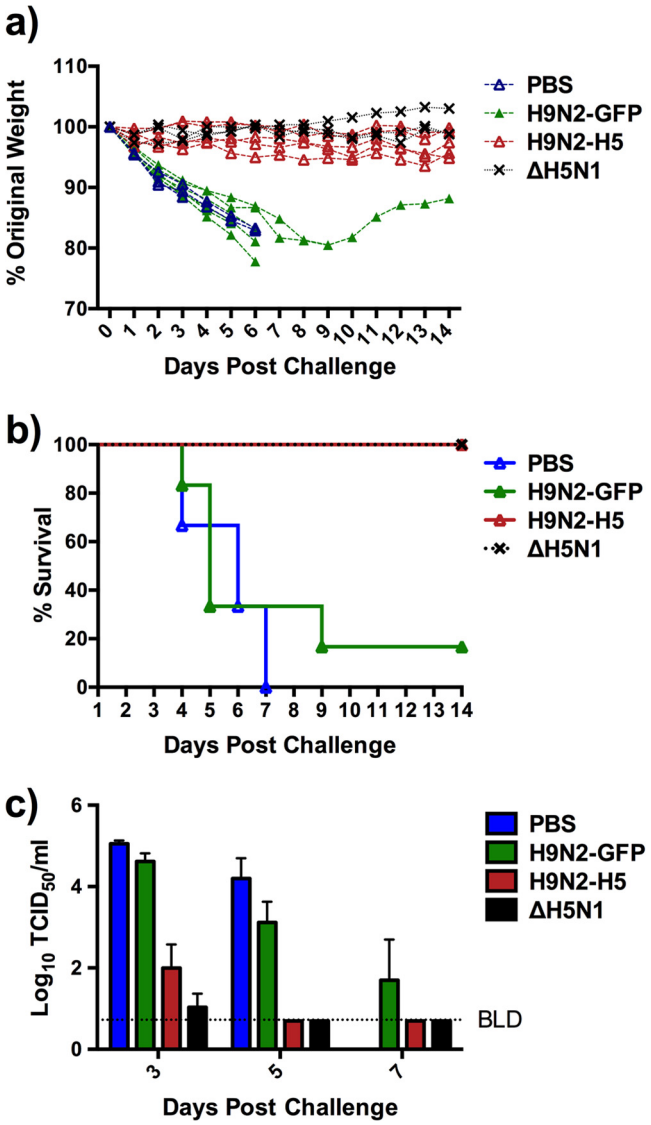

FIG 5 Protective efficacy of the H9N2-H5 rearranged influenza virus vector in ferrets. Three- to six-month-old female ferrets ($n = 6$/group) were vaccinated intranasally with 10^6 EID_{50}/ferret of the recombinant viruses and boosted 2 weeks later using the same virus and dose. Four groups were included: one group received the H9N2-H5 vaccine, one group received the H9N2-GFP heterologous control, one group received the ΔH5N1 homologous control, and one group was mock vaccinated with PBS. Prior to challenge, one ferret in the H9N2-H5-vaccinated group died due to unknown etiology. Two weeks after boost, ferrets were challenged with 10^6 EID_{50}/ferret (equivalent to 10,000 FLD_{50}) of H5N1, and protection was evaluated. (a) Body weight was monitored daily, and the percent change over the original body weight at the time of challenge is shown. (b) Likewise, survival upon challenge was monitored daily. (c) Nasal washes were collected daily for 9 days following challenge to assess challenge virus shedding. Virus shedding in nasal secretions is presented as the mean ± standard deviation of the $\log_{10}$ $TCID_{50}$/ml. The lower limit of detection was 0.6 $TCID_{50}$/ml.

seroconversion based on an enzyme-linked immunosorbent assay (ELISA) against the viral NP antigen and neutralizing antibodies against H9, it was not possible to correlate protection with the levels of circulating H5 neutralizing antibodies in vaccinated animals (Tables 2 and 3 and data not shown). This finding is not unique to this vaccine study, since multiple studies have shown poor humoral responses after vaccination against H5N1 when using inactivated, vectored, or live-attenuated vaccines (29–32). Collectively, the mouse and ferrets studies suggest that the rearranged H9N2-H5 vector can elicit efficient protection against avian H5 and H9 viruses.

DISCUSSION

We rearranged the genome of IAV with the goal of expanding its genome coding capacity and improving its stability. Using this strategy, we successfully rescued rearranged IAVs carrying up to 1.7 kb of foreign sequence (H5 HA ORF). Interestingly, stable viruses expressing GFP and GLuc reporters were also recovered, demonstrating that the cytosolic and secretory pathways can be accessed using this technology.

The impaired growth of the rearranged viruses could be explained mechanistically by the lower polymerase activity displayed by the PB1-2A-NEP/NS2 compared to the wt PB1 gene. The mechanisms responsible for these phenotypes are not completely understood. We previously showed that incorporating an eight-amino-acid HA tag in the C terminus of PB1 reduced viral replication and polymerase activity (13, 18). It is possible that the 18-amino-aci-long FMDV 2A tag in PB1 contributes to the attenuated polymerase activity and viral growth. Additionally, expression of NEP/NS2 from a single ORF in segment 2 may alter the levels of transcription and replication of the rearranged virus relative to their wt counterparts. NEP/NS2 has been shown to modulate the relative amounts of influenza virus cRNA, vRNA, and mRNA (20). Lastly, the exact boundaries of the packaging signals for IAV are not yet properly defined and may be subtype or even strain specific. In this study, rearranged H9N2 IAV vectors were engineered with respect for the length of packaging signals previ-

TABLE 2 The NP-blocking ELISA on pre-HPAI H5N1 challenge serum showed all LAIV-vaccinated animals were positive for NP antibodies[a]

Group	Animal no.	NP blocking ELISA S/N ratio	Result
H9N2-GFP	709	0.141	+
	710	0.169	+
	711	0.134	+
	712	0.169	+
	713	0.180	+
	714	0.190	+
H9N2-H5	715	0.171	+
	716	0.191	+
	718	0.124	+
	719	0.143	+
	720	0.138	+
PBS	721	0.651	−
	722	0.646	−
	723	0.727	−
ΔH5N1	724	0.141	+
	725	0.148	+
	726	0.131	+

[a] Serum was obtained from animals 13 days post-boost vaccination. NP ELISA titers were determined by using the Flu Detect BE kit (avian influenza virus antibody test kit; cELISA) from Synbiotics (College Park, MD), following the manufacturer's directions. A signal-to-noise (S/N) ratio of less than 0.6 was considered positive for antibody against influenza virus.

TABLE 3 H9 and H5 HI results for pre-HPAI H5N1 challenge serum from LAIV-vaccinated ferrets[a]

Group	Animal no.	H9 HI titer	H5 HI titer
H9N2-GFP	709	160	<10
	710	320	<10
	711	320	<10
	712	320	<10
	713	160	<10
	714	320	<10
H9N2-H5	715	80	<10
	716	40	<10
	718	80	10
	719	80	10
	720	160	<10
PBS	721	<10	<10
	722	<10	<10
	723	<10	<10
ΔH5N1	724	<10	40
	725	<10	20
	726	<10	<10

[a] Serum was obtained from animals 13 days post-boost vaccination. Serum samples were treated with receptor-destroying enzyme (Accurate Chemical and Scientific Corp., Westbury, NY) to remove nonspecific receptors, and the antiviral antibody titers were evaluated using an HI assay as outlined in the WHO *Manual for the Laboratory Diagnosis and Virological Surveillance of Influenza* (28). H9N2 wt and ΔH5N1 were used in these assays. HI titers are reported as the reciprocal of the highest dilution of serum that showed activity against the corresponding virus. HI titers for each animal are shown. The limit of detection for this technique is 10.

ously reported for H1N1 strains (17). Fine mapping of the optimum *cis*-acting sequences required for H9N2 vRNA incorporation into influenza virus particles may allow improvements in virus yield and stability of foreign genes. Further studies into the mechanisms of attenuation of rearranged IAV may shed light onto basic molecular constraints that control IAV replication.

As a proof of principle for the rearranged influenza virus vector platform, we expressed the entire H5 HA ORF in the eighth segment of the rearranged H9N2 IAV vector and tested the safety and the efficacy of this vector in protection against H5 and H9 viruses. The rearranged viruses were innocuous after administration in both mice and ferrets, and the rearrangement itself attenuated an otherwise HPAIV H5N1 virus in chickens. The H9N2-H5 vaccine proved to be very efficacious against robust challenges with HPAIV H5N1 and a transmissible avian H9:pH1N1 reassortant. Unlike the LAIVs that are currently licensed in the United States, which are based on a few point mutations that are not sufficient to attenuate H9N2 wt (13, 21, 33), genome rearrangement may allow a more stable attenuation phenotype, since it involves more dramatic changes in the structure of the IAV genome.

In summary, IAVs are amenable to genome rearrangement and can accommodate large pieces of additional genetic material while preserving replication and immunogenicity. This vaccine is safe, does not require expensive high-containment manufacturing facilities, and can be grown in eggs, the substrate of choice for producing IAV vaccines. Development of this technology may pave the way for a novel class of influenza virus vectors that can provide immunity not only to influenza virus but also against other diseases.

ACKNOWLEDGMENTS

We thank Andrea Ferrero, Yonas Araya, Qion Chen, and Johanna Lavigne for their technical assistance.

This research was made possible through funding by NIAID, NIH, contract HHSN266200700010C.

L.P. designed the cloning strategy, recovered viruses by reverse genetics, performed *in vitro* experiments and mouse studies, interpreted the data, and wrote the manuscript. T.S. designed and performed ferret studies, hemagglutination inhibition (HI) assays, and ELISAs, interpreted the data, and cowrote the manuscript. A.C., S.K., and M.A. performed and/or assisted with experiments and/or interpreted the data. H.S. performed IFA. H.C. and W.L. performed Western blot analysis and interpreted data. D.R.P. invented the rearranged genome strategy, designed the study, interpreted the data, and wrote and edited the manuscript.

The University of Maryland has submitted a provisional patent application covering the use of rearranged influenza viruses.

REFERENCES

1. **Draper SJ, Heeney JL.** 2010. Viruses as vaccine vectors for infectious diseases and cancer. Nat. Rev. Microbiol. **8**:62–73.
2. **Hoffmann E, Neumann G, Kawaoka Y, Hobom G, Webster RG.** 2000. A DNA transfection system for generation of influenza A virus from eight plasmids. Proc. Natl. Acad. Sci. U. S. A. **97**:6108–6113.
3. **Garulli B, Kawaoka Y, Castrucci MR.** 2004. Mucosal and systemic immune responses to a human immunodeficiency virus type 1 epitope induced upon vaginal infection with a recombinant influenza A virus. J. Virol. **78**:1020–1025.
4. **Fouchier RA, Munster V, Wallensten A, Bestebroer TM, Herfst S, Smith D, Rimmelzwaan GF, Olsen B, Osterhaus AD.** 2005. Characterization of a novel influenza A virus hemagglutinin subtype (H16) obtained from black-headed gulls. J. Virol. **79**:2814–2822.
5. **Belshe RB, Edwards KM, Vesikari T, Black SV, Walker RE, Hultquist M, Kemble G, Connor EM; CAIV-T Comparative Efficacy Study Group.** 2007. Live attenuated versus inactivated influenza vaccine in infants and young children. N. Engl. J. Med. **356**:685–696.
6. **Martínez-Sobrido L, García-Sastre A.** 2007. Recombinant influenza virus vectors. Future Virol. **2**:401–416.
7. **WHO.** 2010. Antigenic and genetic characteristics of influenza A (H5N1) and influenza A (H9N2) viruses and candidate vaccine viruses developed for potential use in human vaccines. World Health Organization, Geneva, Switzerland.
8. **Belshe RB, Mendelman PM, Treanor J, King J, Gruber WC, Piedra P, Bernstein DI, Hayden FG, Kotloff K, Zangwill K, Iacuzio D, Wolff M.** 1998. The efficacy of live attenuated, cold-adapted, trivalent, intranasal influenzavirus vaccine in children. N. Engl. J. Med. **338**:1405–1412.
9. **Johnson PR, Jr, Feldman S, Thompson JM, Mahoney JD, Wright PF.** 1985. Comparison of long-term systemic and secretory antibody responses in children given live, attenuated, or inactivated influenza A vaccine. J. Med. Virol. **17**:325–335.
10. **Suguitan AL, Jr, McAuliffe J, Mills KL, Jin H, Duke G, Lu B, Luke CJ, Murphy B, Swayne DE, Kemble G, Subbarao K.** 2006. Live, attenuated influenza A H5N1 candidate vaccines provide broad cross-protection in mice and ferrets. PLoS Med. **3**:e360. doi:10.1371/journal.pmed.0030360.
11. **Treanor JJ, Campbell JD, Zangwill KM, Rowe T, Wolff M.** 2006. Safety and immunogenicity of an inactivated subvirion influenza A (H5N1) vaccine. N. Engl. J. Med. **354**:1343–1351.
12. **Kimble JB, Sorrell E, Shao H, Martin PL, Perez DR.** 2011. Compatibility of H9N2 avian influenza surface genes and 2009 pandemic H1N1 internal genes for transmission in the ferret model. Proc. Natl. Acad. Sci. U. S. A. **108**:12084–12088.
13. **Song H, Nieto GR, Perez DR.** 2007. A new generation of modified live-attenuated avian influenza viruses using a two-strategy combination as potential vaccine candidates. J. Virol. **81**:9238–9248.
14. **Neumann G, Hughes MT, Kawaoka Y.** 2000. Influenza A virus NS2 protein mediates vRNP nuclear export through NES-independent interaction with hCRM1. EMBO J. **19**:6751–6758.
15. **de Felipe P.** 2004. Skipping the co-expression problem: the new 2A "CHYSEL" technology. Genet. Vaccines Ther. **2**:13. doi:10.1186/1479-0556-2-13.
16. **Fujii K, Fujii Y, Noda T, Muramoto Y, Watanabe T, Takada A, Goto H,**

Horimoto T, Kawaoka Y. 2005. Importance of both the coding and the segment-specific noncoding regions of the influenza A virus NS segment for its efficient incorporation into virions. J. Virol. **79**:3766–3774.
17. **Liang Y, Hong Y, Parslow TG.** 2005. *cis*-acting packaging signals in the influenza virus PB1, PB2, and PA genomic RNA segments. J. Virol. **79**: 10348–10355.
18. **Pena L, Vincent AL, Ye J, Ciacci-Zanella JR, Angel M, Lorusso A, Gauger PC, Janke BH, Loving CL, Perez DR.** 2011. Modifications in the polymerase genes of a swine-like triple-reassortant influenza virus to generate live attenuated vaccines against 2009 pandemic H1N1 viruses. J. Virol. **85**:456–469.
19. **Golde WT, Gollobin P, Rodriguez LL.** 2005. A rapid, simple, and humane method for submandibular bleeding of mice using a lancet. Lab. Anim. (NY) **34**:39–43.
20. **Robb NC, Smith M, Vreede FT, Fodor E.** 2009. NS2/NEP protein regulates transcription and replication of the influenza virus RNA genome. J. Gen. Virol. **90**:1398–1407.
21. **Hickman D, Hossain MJ, Song H, Araya Y, Solorzano A, Perez DR.** 2008. An avian live attenuated master backbone for potential use in epidemic and pandemic influenza vaccines. J. Gen. Virol. **89**:2682–2690.
22. **Solorzano A, Ye J, Perez DR.** 2010. Alternative live-attenuated influenza vaccines based on modifications in the polymerase genes protect against epidemic and pandemic flu. J. Virol. **84**:4587–4596.
23. **Basler CF, Aguilar PV.** 2008. Progress in identifying virulence determinants of the 1918 H1N1 and the southeast Asian H5N1 influenza A viruses. Antiviral Res. **79**:166–178.
24. **Gao Q, Lowen AC, Wang TT, Palese P.** 2010. A nine-segment influenza a virus carrying subtype H1 and H3 hemagglutinins. J. Virol. **84**:8062–8071.
25. **Gao Q, Palese P.** 2009. Rewiring the RNAs of influenza virus to prevent reassortment. Proc. Natl. Acad. Sci. U. S. A. **106**:15891–15896.
26. **Matsuoka Y, Lamirande EW, Subbarao K.** 2009. The ferret model for influenza. Curr. Protoc. Microbiol. **Chapter 15:**Unit 15G.12.
27. **Mahmood K, Bright RA, Mytle N, Carter DM, Crevar CJ, Achenbach JE, Heaton PM, Tumpey TM, Ross TM.** 2008. H5N1 VLP vaccine induced protection in ferrets against lethal challenge with highly pathogenic H5N1 influenza viruses. Vaccine **26**:5393–5399.
28. **WHO.** 2011. Manual for the laboratory diagnosis and virological surveillance of influenza. World Health Organization, Geneva, Switzerland.
29. **Banner D, Kelvin AA.** 2012. The current state of H5N1 vaccines and the use of the ferret model for influenza therapeutic and prophylactic development. J. Infect. Dev. Ctries. **6**:465–469.
30. **El Sahly HM, Keitel WA.** 2008. Pandemic H5N1 influenza vaccine development: an update. Expert Rev. Vaccines **7**:241–247.
31. **Zhang J.** 2012. Advances and future challenges in recombinant adenoviral vectored H5N1 influenza vaccines. Viruses **4**:2711–2735.
32. **Zheng D, Yi Y, Chen Z.** 2012. Development of live-attenuated influenza vaccines against outbreaks of H5N1 influenza. Viruses **4**:3589–3605.
33. **Jin H, Lu B, Zhou H, Ma C, Zhao J, Yang CF, Kemble G, Greenberg H.** 2003. Multiple amino acid residues confer temperature sensitivity to human influenza virus vaccine strains (FluMist) derived from cold-adapted A/Ann Arbor/6/60. Virology **306**:18–24.